

# Energy Flux Paths in Lakes and Reservoirs

Sofya Guseva <sup>1,\*</sup>, Peter Casper <sup>2</sup>, Torsten Sachs <sup>3</sup>, Uwe Spank <sup>4</sup> and Andreas Lorke <sup>1</sup>

<sup>1</sup> Institute for Environmental Sciences, University of Koblenz-Landau, 76829 Landau, Germany; lorke@uni-landau.de

<sup>2</sup> Department of Experimental Limnology, Leibniz-Institute of Freshwater Ecology and Inland Fisheries, 12587 Berlin, Germany; pc@igb-berlin.de

<sup>3</sup> GFZ German Research Centre for Geosciences, 14473 Potsdam, Germany; torsten.sachs@gfz-potsdam.de

<sup>4</sup> Institute of Hydrology and Meteorology, Chair of Meteorology, Technische Universität Dresden, 01069 Dresden, Germany; Uwe.Spank@tu-dresden.de

\* Correspondence: guseva@uni-landau.de

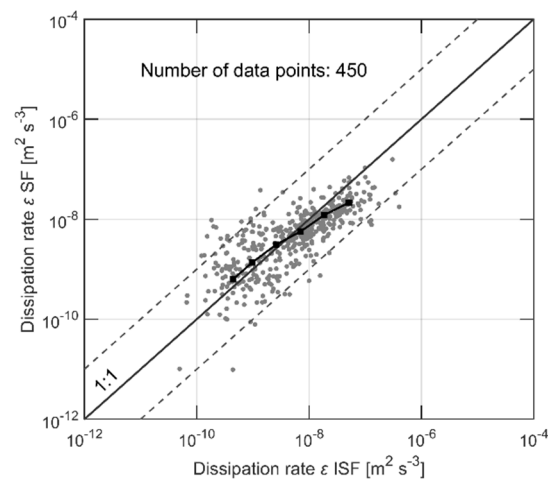


**Figure S1.** Dissipation rate estimated using structure function method (SF) versus dissipation rate calculated using inertial subrange fitting method (ISF) at ~1.5 m depth for measurements in Bautzen Reservoir (gray dots). Both dissipation rates are quality checked (see Section 2.5). The black line with squares shows the bin-average dissipation rates. The gray solid line represents a 1:1 relationship, dashed gray lines mark one order of magnitude deviations.

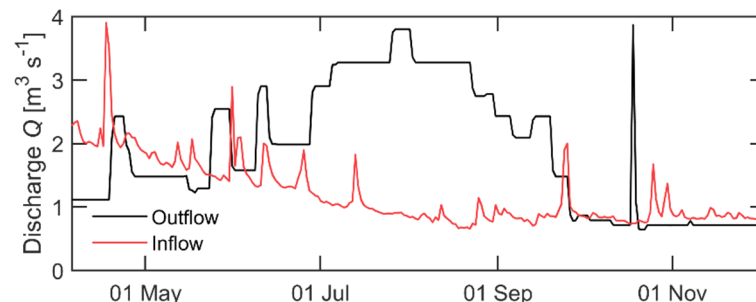


**Figure S2.** Discharge of the inflow (red line) and outflow (at the outlet tower) of Bautzen reservoir. The data was provided by the the Landestalsperren-Verwaltung Sachsen (LTV).

**Citation:** Guseva, S.; Casper, P.; Sachs, T.; Spank, U.; Lorke, A. Energy Flux Paths in Lakes and Reservoirs. *Water* **2021**, *13*, 3270. <https://doi.org/10.3390/w13223270>

Academic Editor: Lars Bengtsson

Received: 06 August 2021

Accepted: 10 November 2021

Published: 18 November 2021

**Publisher's Note:** MDPI stays neutral with regard to jurisdictional claims in published maps and institutional affiliations.



**Copyright:** © 2021 by the authors. Licensee MDPI, Basel, Switzerland. This article is an open access article distributed under the terms and conditions of the Creative Commons Attribution (CC BY) license (<http://creativecommons.org/licenses/by/4.0/>).

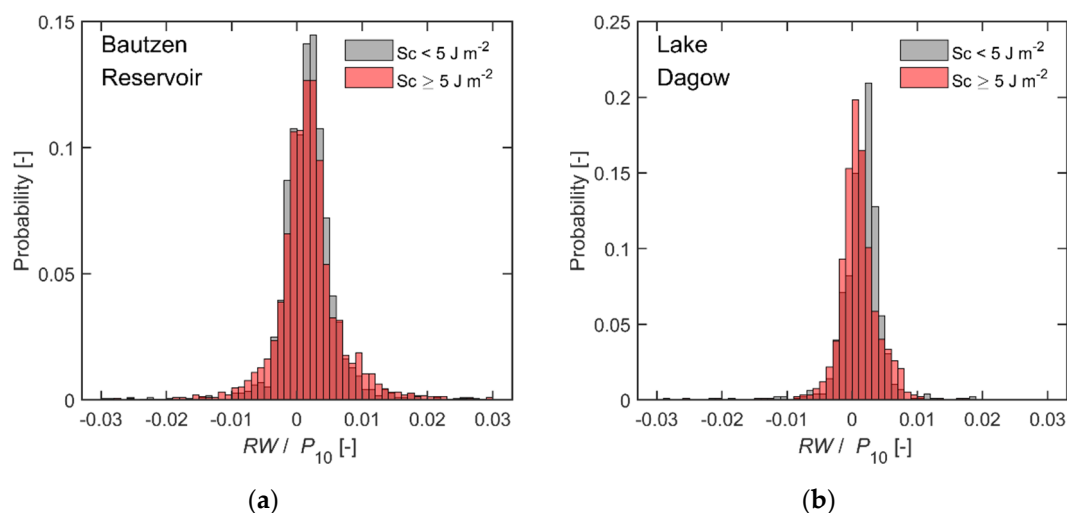


**Figure S3.** Probability distribution of the ratio of rate of working ( $RW$ ) to wind energy flux ( $P_{10}$ ) selected for two cases: Schmidt stability ( $Sc$ )  $< 5 \text{ J m}^{-2}$  (area shown in gray, corresponding to non-stratified conditions) and  $Sc \geq 5 \text{ J m}^{-2}$  (area shown in red, corresponding to stratified conditions) for (a) Bautzen Reservoir. The median values are  $1.8 \times 10^{-3}$  and  $1.6 \times 10^{-3}$ , the average values ( $\pm$  standard deviation) are  $(2 \pm 4) \cdot 10^{-3}$  and  $(0.6 \pm 21.6) \cdot 10^{-2}$ , for non-stratified and stratified conditions, respectively. (b) Lake Dagow. The median values are  $1.7 \times 10^{-3}$  and  $0.7 \times 10^{-3}$  and average values of  $(1.3 \pm 4.5) \times 10^{-3}$  and  $(1.1 \pm 4.2) \times 10^{-3}$  for non-stratified and stratified conditions, respectively.

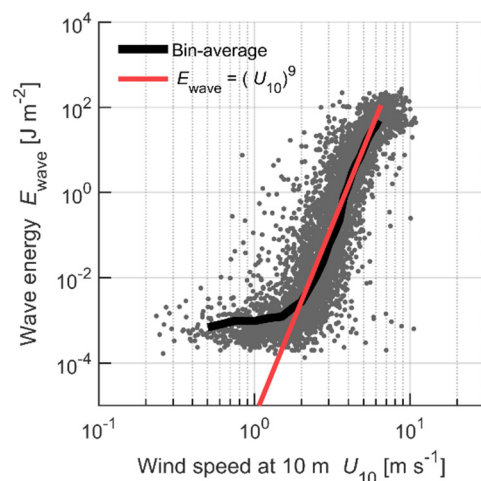


**Figure S4.** Surface wave energy versus wind speed at 10 m height at the platform location in Bautzen Reservoir (gray dots). Wave energy shows strong dependence on wind speed exceeding 2–3  $\text{m s}^{-1}$ . The black line shows bin-average data, the red line represents a power-law relationship with an exponent of nine. The latter was obtained from a linear regression of log-transformed data.

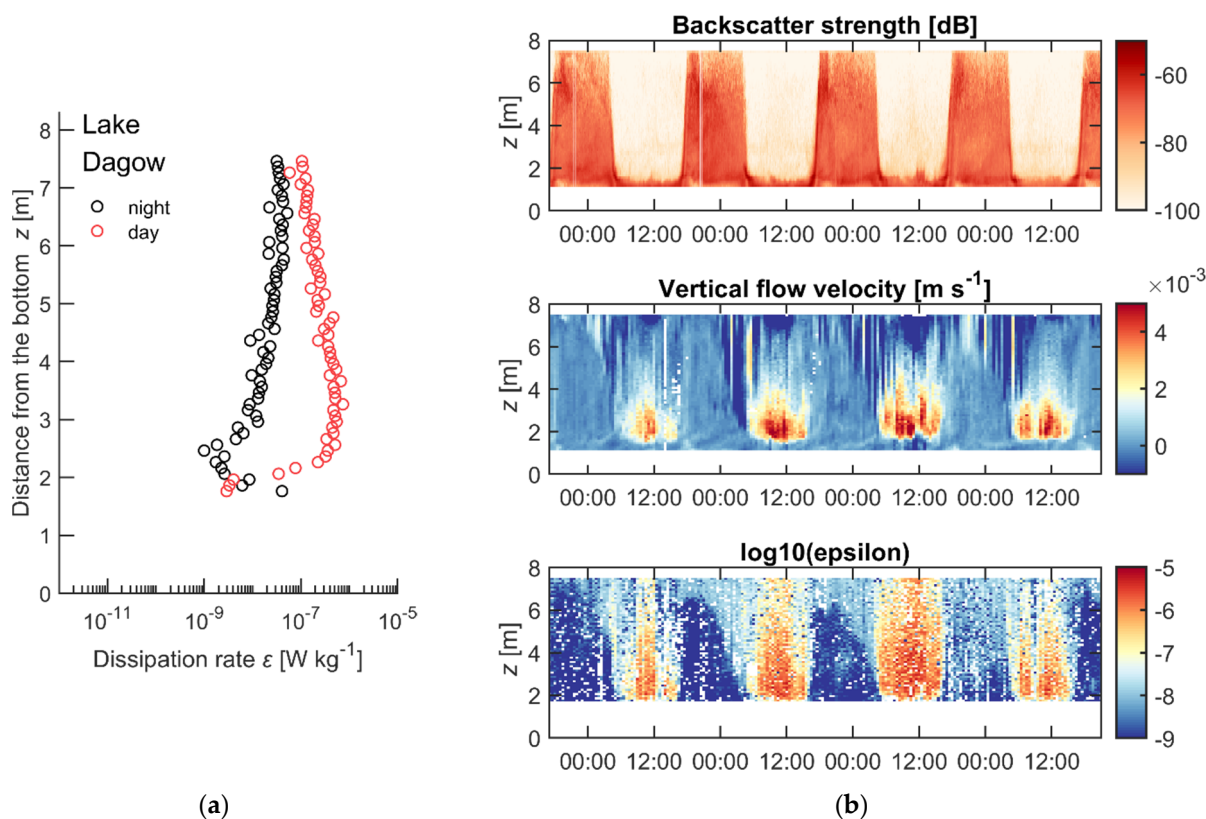


**Figure S5.** (a) Dissipation rates of turbulent kinetic energy averaged over night and over daytime during the first ADCP deployment in Lake Dagow. (b) Acoustic backscatter strength recorded by the ADCP (upper panel), vertical flow velocity (middle panel), dissipation rate (lower panel). High magnitudes of backscatter strength indicate high concentration of scattering particles, including zooplankton, performing a diel vertical migration with high daytime concentration at bottom and higher concentrations over the entire water column during night. High vertical flow velocity and dissipation rates during the day does not coincide with organism’s activity. However, starting from midnight we see a “trace” in dissipation rates which possibly indicate the time period when the species begin move towards the bottom.

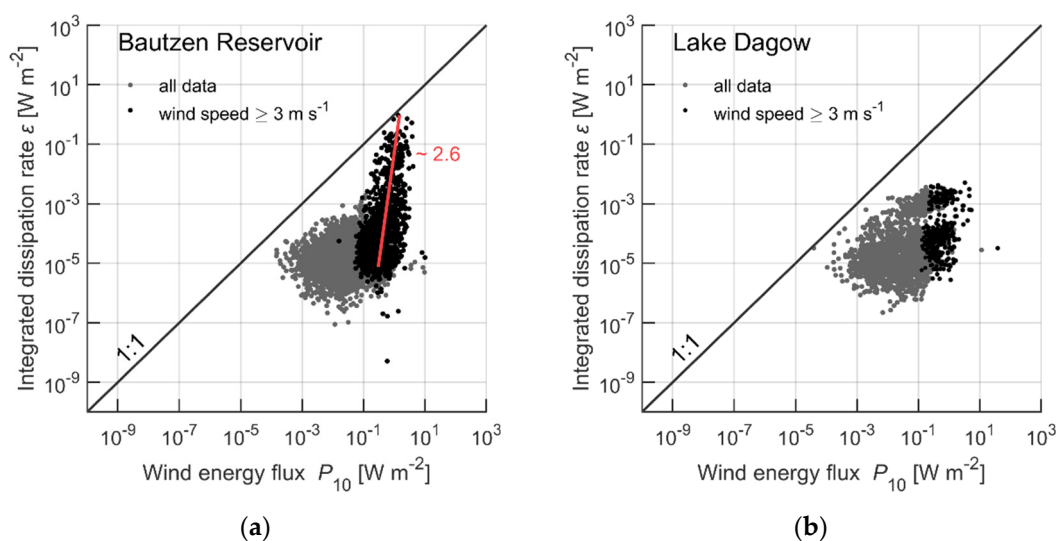


**Figure S6.** Depth-integrated dissipation rate (including surface and bottom boundary layers and interior of the water bodies) versus the vertical wind energy flux above the water surface in (a) Bautzen Reservoir; (b) Lake Dagow. Gray dots indicate all data, black dots show the data points corresponding to the wind speed exceeding  $3 \text{ m s}^{-1}$ . The gray solid line represents a 1:1 relationship, the red line in (a) indicates power-law relationship with an exponent of  $\sim 2.6$ .

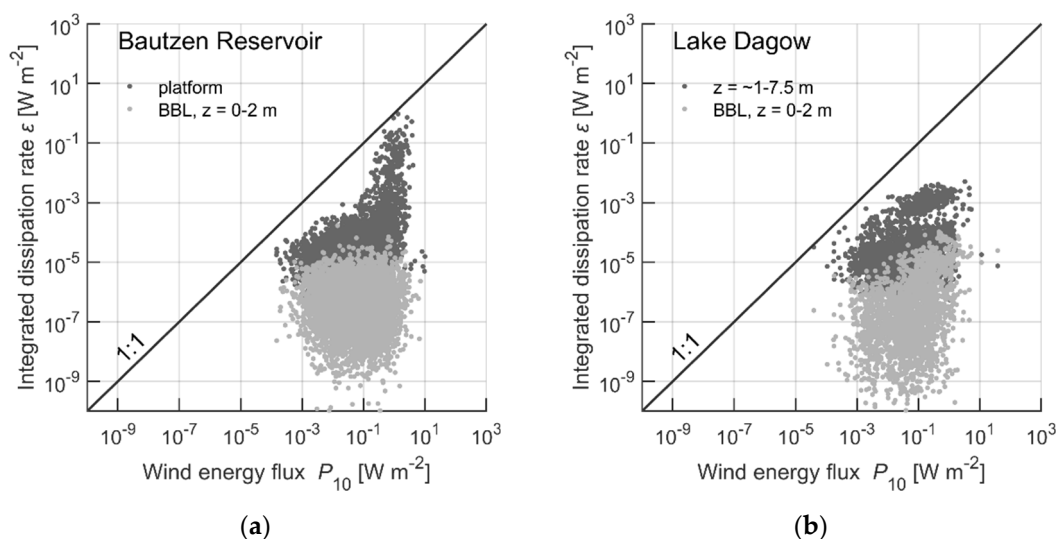


**Figure S7.** Dissipation rate integrated over the bottom boundary layer (the thickness of 2 m, light gray dots) and over the rest of the water column where the ADCP measurements are available (dark gray dots) using data from (a) Bautzen Reservoir; (b) Lake Dagow. The gray solid line represents a 1:1 relationship.

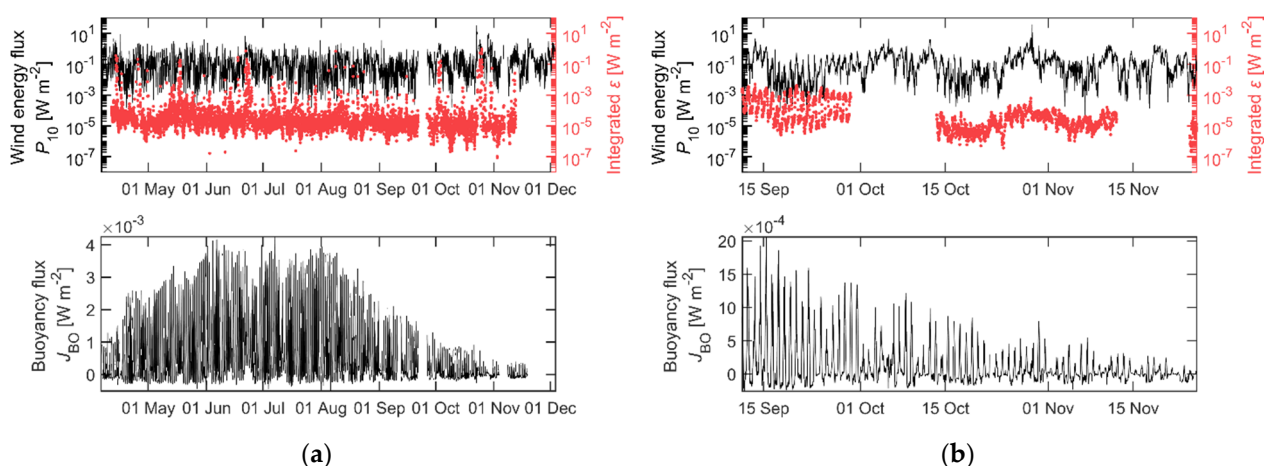


**Figure S8.** Temporal dynamics of wind energy flux (black line, upper panel), dissipation rates integrated over the water depth (red dots, upper panel) and buoyancy flux (lower panel) for data measured in (a) Bautzen Reservoir; (b) Lake Dagow. Note the pronounced diurnal pattern in integrated energy dissipation rates in Lake Dagow during the first ADCP deployment (cf. Figure S4).

Table S1. Energy content and energy fluxes

Energy fluxes (W m <sup>-2</sup> )		Minimum	Average or log-average	Maximum	Standard Deviation <sup>1</sup>	% from P <sub>10</sub>
Wind energy flux P <sub>10</sub>	Bautzen Reser- voir	1.5 × 10 <sup>-4</sup>	7.4 × 10 <sup>-2</sup>	32		100
	Lake Dagow	3.9 × 10 <sup>-5</sup>	6.2 × 10 <sup>-2</sup>	38		
Wave energy flux P <sub>wave</sub> (W m <sup>-1</sup> )	Bautzen Reservoir	2.3 × 10 <sup>-4</sup> , 1.7 × 10 <sup>-4</sup>	0.84, 40	23, 1292	2.3, 126	
	Lake Dagow	1.7 × 10 <sup>-4</sup>	0.08	12	0.44	
Surface heat flux H <sub>net</sub>	Bautzen Reservoir	-155	173	1113	266	
	Lake Dagow	-130	43	763	121	
Buoyancy flux B	Bautzen Reservoir	-5.1 × 10 <sup>-4</sup>	6.1 × 10 <sup>-4</sup>	4.2 × 10 <sup>-3</sup>		
	Lake Dagow	-2.6 × 10 <sup>-4</sup>	1.1 × 10 <sup>-4</sup>	2.1 × 10 <sup>-3</sup>		
Depth-inte- grated dissipa- tion rate ε	Bautzen Reservoir	4.4 × 10 <sup>-11</sup>	1.7 × 10 <sup>-5</sup>	9.5 × 10 <sup>-1</sup>		0.23
	Lake Dagow	2.2 × 10 <sup>-7</sup>	3.4 × 10 <sup>-5</sup>	5.1 × 10 <sup>-3</sup>		0.5
Energy content (J m <sup>-2</sup> )						
Schmidt stability	Bautzen Reser- voir	0	41.8	177.5	44.5	
	Lake Dagow	0.7	4.3	21.2	4.6	
Surface waves	Bautzen Reservoir	1.7 × 10 <sup>-4</sup> , 1.4 × 10 <sup>-4</sup>	0.04, 0.3	21, 907	2, 93	0.5, 4
	Lake Dagow	1.7 × 10 <sup>-4</sup>	0.02	11	0.43	0.5
Basin-scale internal waves	Bautzen Reservoir	0.1	2.4	12.8	2	0.008–0.09 (average 0.04)
	Lake Dagow		0.1			0.002
High-frequency internal waves	Bautzen Reservoir	8.7 × 10 <sup>-4</sup>	0.1	0.9	0.1	
	Lake Dagow		0.1			

<sup>1</sup> Standard deviation is not defined for the parameters with lognormal distribution.